Environmental Science & Technology

Article

pubs.acs.org/est

Modeling the Current and Future Roles of Particulate Organic Nitrates in the Southeastern United States

Havala O. T. Pye,[*,†] Deborah J. Luecken,[†] Lu Xu,[‡] Christopher M. Boyd,[‡] Nga L. Ng,[‡,§] Kirk R. Baker,[⊥] Benjamin R. Ayres,[∥] Jesse O. Bash,[†] Karsten Baumann,[#] William P. L. Carter,[∇] Eric Edgerton,[#] Juliane L. Fry,[∥] William T. Hutzell,[†] Donna B. Schwede,[†] and Paul B. Shepson[○]

[†]National Exposure Research Laboratory, U.S. Environmental Protection Agency, Research Triangle Park, North Carolina 27711, United States

[‡]School of Chemical and Biomolecular Engineering, Georgia Institute of Technology, Atlanta, Georgia 30332, United States

[§]School of Earth and Atmospheric Sciences, Georgia Institute of Technology, Atlanta, Georgia 30332, United States

[⊥]Office of Air Quality Planning and Standards, U.S. Environmental Protection Agency, Research Triangle Park, North Carolina 27711, United States

[∥]Department of Chemistry, Reed College, Portland, Oregon 97202, United States

[#]Atmospheric Research and Analysis, Inc., Cary, North Carolina 27513, United States

[∇]College of Engineering, Center for Environmental Research and Technology, University of California at Riverside, Riverside, California 92512, United States

[○]Department of Chemistry, Purdue University, West Lafayette, Indiana 47907, United States

Supporting Information

ABSTRACT: Organic nitrates are an important aerosol constituent in locations where biogenic hydrocarbon emissions mix with anthropogenic NO_x sources. While regional and global chemical transport models may include a representation of organic aerosol from monoterpene reactions with nitrate radicals (the primary source of particle-phase organic nitrates in the Southeast United States), secondary organic aerosol (SOA) models can underestimate yields. Furthermore, SOA parametrizations do not explicitly take into account organic nitrate compounds produced in the gas phase. In this work, we developed a coupled gas and aerosol system to describe the formation and subsequent aerosol-phase partitioning of organic nitrates from isoprene and monoterpenes with a focus on the Southeast United States. The concentrations of organic aerosol and gas-phase organic nitrates were improved when particulate organic nitrates were assumed to undergo rapid (τ = 3 h) pseudohydrolysis resulting in nitric acid and nonvolatile secondary organic aerosol. In addition, up to 60% of less oxidized-oxygenated organic aerosol (LO-OOA) could be accounted for via organic nitrate mediated chemistry during the Southern Oxidants and Aerosol Study (SOAS). A 25% reduction in nitrogen oxide (NO + NO_2) emissions was predicted to cause a 9% reduction in organic aerosol for June 2013 SOAS conditions at Centreville, Alabama.

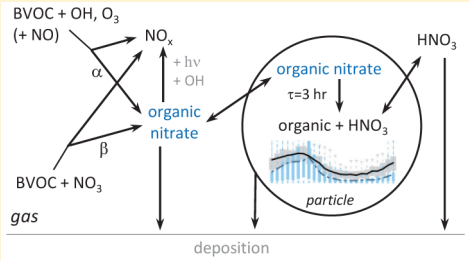

INTRODUCTION

In locations such as the Southeast United States, biogenic emissions mix with emissions from vehicles, power plants, and industrial sources. This mix of atmospheric constituents produces particles with implications for human health, ecosystems, visibility, and climate. Major contributors to particulate matter (PM) mass in the Southeast U.S. include sulfate and organics which are generally comparable in magnitude.[1] Aerosol concentrations have decreased since the early 2000s as a result of anthropogenic emission reductions with sulfate decreasing to a greater extent than organic carbon.[1] As organic carbon becomes a larger fraction of total PM, understanding the past, current, and future contributors to organic aerosol (OA) in the Southeast U.S. is important.

Organic nitrates (ON) are a significant component of PM mass in multiple places across the United States including California, Colorado, Alabama, and Georgia.[2−8] Most particle-phase organic nitrates (pON) in the Southeast U.S. are attributable to monoterpene oxidation,[4,9] and this aerosol represents an anthropogenic control on biogenic secondary organic aerosol (SOA) since it requires gas-phase nitrogen oxides to be produced. Nitrate radical (NO_3) oxidation of monoterpenes results in high yields of organic nitrates and this pathway has been shown to account for more than half of the

Received: August 3, 2015
Revised: November 4, 2015
Accepted: November 6, 2015
Published: November 6, 2015

ACS Publications © 2015 American Chemical Society

DOI: 10.1021/acs.est.5b03738
Environ. Sci. Technol. 2015, 49, 14195−14203

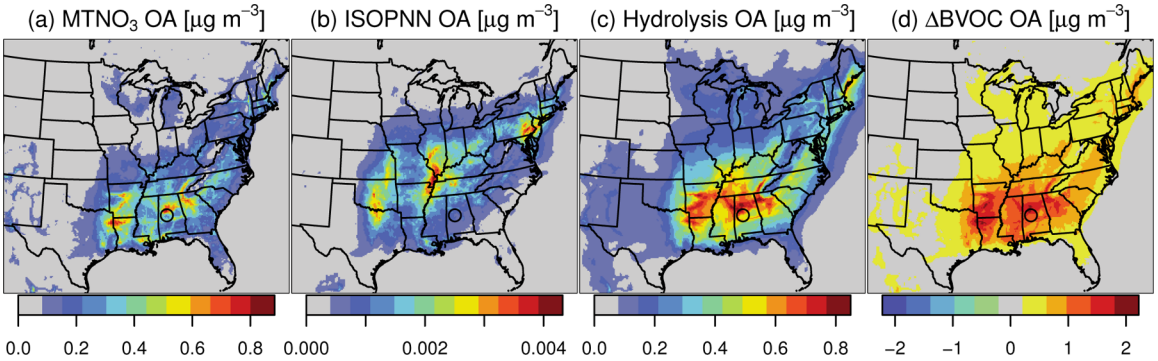

Figure 1. Predicted concentration (a) of monoterpene nitrate SOA, (b) of isoprene nitrate SOA, (c) of SOA from hydrolysis of nitrates, and (d) change in BVOC SOA compared to base CMAQ v5.0.2+[54,57] without explicit pON SOA. τ = 3 h pseudohydrolysis. The SOAS CTR ground site is indicated.

monoterpene SOA in the U.S.[10] and double SOA in polluted areas.[11] This route to SOA is primarily (but not exclusively) active during the night as NO_3 efficiently photolyzes during the day. Reactions of β-pinene, Δ-3-carene, and limonene with NO_3 have gas-phase organic nitrate yields ranging from 30 to 74%[12−15] and aerosol yields up to 100%.[16] During the day, oxidation by the hydroxyl radical (OH) or ozone (O_3) also produces organic nitrates under RO_2 + NO conditions.

The fate of particle-phase organic nitrates is uncertain and determines whether pON is a temporary or terminal sink for NO_x with potential implications for ozone.[17−19] Particle-phase nitrates may deposit, return to the gas phase where they can release NO_x, or participate in a particle-phase reaction. Tertiary nitrates undergo fast hydrolysis with time scales on the order of hours[16,20] to minutes,[21] whereas primary and secondary nitrates are thought to be relatively stable.[22] Rapid conversion of pON to alcohols or other species may cause the contribution of nitrogen mediated aerosol to be underestimated in ambient observations,[23] particularly under acidic conditions.[22,24]

The Southeast Atmosphere Study (SAS) took place during the summer of 2013 and included the Southern Oxidant and Aerosol Study (SOAS) based in Brent, AL at the Centreville (CTR) SouthEastern Aerosol Research and Characterization (SEARCH) Network site. CTR is a regionally representative rural site to the southwest of Birmingham, Alabama.[1,25] A primary goal of SOAS was to examine interactions between biogenic and anthropogenic systems. As part of SOAS, positive matrix factorization (PMF) analysis of ambient data sets identified a component of aerosol related to organic nitrates.[4] This component, LO-OOA, or less-oxygenated-oxidized organic aerosol is 20−30% organic nitrates with additional mass contributions from other sources and species. LO-OOA is the second largest contributer to brown carbon absorption (after biomass burning)[26] and accounts for 19−34% of total OA mass in the Southeast in summer and winter.[4] In this work, we used the Community Multiscale Air Quality (CMAQ) model[27] to develop a representation of pON-derived aerosol (aerosol from organic nitrates and their reaction products) and evaluated it using measurements from the SOAS campaign. We also examined how reductions in NO_x (NO + NO_2) emissions are predicted to affect organic aerosol in the southeastern United States.

■ METHODS

Chemical Transport Model. Conditions over the eastern United States were simulated using the CMAQ model[27] (available through www.cmascenter.org) to overlap with the SOAS field campaign (see Figure 1 for the horizontal domain). The Weather Research and Forecasting model (WRF), Advanced Research WRF core (ARW) model version 3.6.1[28] was applied with a horizontal resolution of 12 km with 35 vertical layers up to a 100 mb for 21 May 2013 through 30 June 2013 to provide meteorological input to CMAQ and the emissions models. Boundary conditions for the 12 km domain were obtained from a 36 km CMAQ simulation with boundary conditions from GEOS-Chem.[29] CMAQ v5.0.2 with additional updates equivalent to CMAQv5.1-beta was used. CMAQv5.1-beta improvements included simultaneous solution of gas and heterogeneous chemical reactions, revisions to in-line photolysis rate calculations, updated aerosol size distribution information,[30] and halogen chemistry over oceans.[31] Additional modifications to CMAQ specific to this study are described in subsequent sections.

Anthropogenic and biogenic emissions were processed using the Sparse Matrix Operator Kernel Emissions (SMOKE) modeling system (www.cmascenter.org/smoke/). Stationary point and area sources were based on iteration 2011v6.1 (generally known as version 1) of the 2011 National Emissions Inventory (NEI).[32] Daily and hourly specific point source emissions from continuous emissions monitoring system (CEMS) were used when available to temporally allocate annual emissions for individual facilities.[33] Mobile source emissions were day specific for the model simulation period based on data submitted to the NEI and generated with SMOKE-MOVES. Solar radiation and temperature estimated with WRF were input to the Biogenic Emission Inventory System (BEIS)[34] version 3.61 along with BELD4 land cover and vegetation speciation information[35] to generate emissions estimates of speciated biogenic compounds. Fire emissions were based on the latest version of the Satellite Mapping Automated Reanalysis Tool for Fire Incident Reconciliation (SMARTFIRE) system (www.airfire.org/smartfire/).

Gas-Phase Chemistry. The gas-phase chemistry used in this work was based on SAPRC07tic mechanism of Xie et al.,[36,37] which is based on SAPRC07t[38] and SAPRC07.[39,40] SAPRC07tic includes a more explicit representation of isoprene and its oxidation products than earlier versions of the chemistry. In particular, it uses separate model species to represent first and second generation isoprene nitrates rather than lumping them with the single RNO3 species used for all other organic nitrates.[36] In this work, SAPRC07tic was further updated to use new reaction rates for isoprene nitrates with OH

DOI: 10.1021/acs.est.5b03738
Environ. Sci. Technol. 2015, 49, 14195−14203

and O_3,[41] revised methacrolein + OH peroxy radical products,[42] and explicit tracking of isoprene dinitrates from isoprene + NO_3. Reaction of isoprene with NO_3 results in about a 70% yield of a first generation isoprene nitrate.[43] A second oxidation by nitrate leads to a semivolatile multifunctional dinitrate, which we called ISOPNN, with a 40% yield.[43] Since isoprene is relatively small in terms of number of carbons, ISOPNN was the only isoprene nitrate from NO_3 oxidation assumed to have a vapor pressure low enough to partition appreciably to particles.

More extensive modifications were made to SAPRC07tic to better represent the gas-phase formation of nitrates from monoterpenes and examine their role as both reservoirs of NO_x and precursors to SOA. The changes only affected model species used to represent the nitrate-containing products, not the underlying SAPRC07 chemistry, assumed branching ratios and product yields, or the model species used for other products. The main change consisted of adding a separate model species to represent organic nitrates formed in monoterpene reactions. This included not only the terpene-derived nitrates represented by RNO3 in SAPRC07tic, but also the nitrate-containing products formed when nitrate-containing peroxy radicals from TERP + NO_3 reacted with HO_2 or other peroxy radicals. Since α-pinene is not expected to form significant aerosol from NO_3 reaction,[44,45] the α-pinene-derived organic nitrates were not explicitly tracked. Some studies do, however, show SOA from α-pinene + NO_3.[14,46,47] The other monoterpenes that are represented by TERP (which include emissions of β-pinene, δ-limonene, α-terpinene, γ-terpinene, camphene, Δ-3-carene, myrcene, pcymene, ocimene, β-phellandrene, sabinene, α-thujene, and terpinolene) form significant aerosol,[12,44] so TERP chemistry was revised to represent organic nitrates separate from lumped RNO3 as a new species: $MTNO_3$.

All monoterpenes in SAPRC07tic form organic nitrates when NO_x is present due to reactions of peroxy radicals with NO. The TERP reactions with OH as represented in SAPRC07 (condensed over multiple generations), produced organic nitrates with a 20.1% net yield:

$$\mathrm{TERP} + \mathrm{OH} \rightarrow \mathrm{TERPRO_2} \tag{1}$$

$$\mathrm{TERPRO_2} + \mathrm{NO} \rightarrow 0.201\mathrm{MTNO_3} + \text{other products} \tag{2}$$

TERP + O_3 also produced peroxy radicals (after formation of a Criegee radical, stabilization, etc.), which resulted in a net yield of $MTNO_3$ of 12.1% under RO_2 + NO conditions.

For TERP + NO_3 reactions, nitrate addition resulted in higher organic nitrate yields:

$$\mathrm{TERP} + \mathrm{NO_3} \rightarrow \mathrm{TERPNRO_2} \tag{3}$$

$$\mathrm{TERPNRO_2} + \mathrm{NO} \rightarrow 0.688\mathrm{MTNO_3} + \text{other products} \tag{4}$$

$$\mathrm{TERPNRO_2} + \mathrm{HO_2} \rightarrow 1.0\mathrm{MTNO_3} \tag{5}$$

$$\mathrm{TERPNRO_2} + \mathrm{NO_3} \rightarrow 0.422\mathrm{MTNO_3} + \text{other products} \tag{6}$$

$$\mathrm{TERPNRO_2} + \mathrm{RO_2} \rightarrow 0.422\delta\mathrm{MTNO_3} + (1-\delta)\mathrm{MTNO_3} + \text{other products} \tag{7}$$

The yield due to NO_3 reaction depended on $TERPNRO_2$ peroxy radical fate and the yield of alkoxy radicals (δ) which was either 50 or 100% for $TERPNRO_2$ + RO_2 depending on the RO_2. Alkoxy radicals formed $MTNO_3$ with a 42.2% yield. The yields through the $TERPNRO_2$ + NO and NO_3 pathways were calculated from estimates of the extent to which the radicals decompose to release NO_2 versus retain the nitrate group.[39,40] Note that the Master Chemical Mechanism (MCM, http://mcm.leeds.ac.uk/MCM) assumes the products from $TERPNRO_2$ + NO or NO_3 decompose and release nitrogen. The yield from the reaction with HO_2 produced 100% hydroperoxide (consistent with MCM[48,49]). To better predict hydroperoxide and nitrate yields, terpene peroxy + HO_2 rate constants were updated to $2.65 \times 10^{-13}\ e^{1300/T}$ (T in K) following MCM v3.3 for a species with 10 carbons.[48,49] This increased the RO_2 + HO_2 reaction rate by a factor of 2.7 at 298 K. This change was only made for peroxy radicals involved in formation of $MTNO_3$.

Heterogeneous conversion of NO_3 to nitric acid using an uptake coefficient of 1.0×10^{-4} (the low range of Mao et al.[50]), nonaromatic changes in SAPRC11,[51] $ClNO_2$ production from N_2O_5,[52] and the latest OH + NO_2 reaction rate constant following IUPAC[53] were added. Deposition of gas-phase nitrates (generally making nitrates more soluble) was also updated. See the Supporting Information for more detail.

Organic Aerosol Treatment. CMAQ v.5.0.2 organic aerosol includes SOA following the scheme of Carlton et al.[54] and remains relatively unchanged since CMAQ v4.7. Semi-volatile aerosol forms via an Odum 2-product parametrization and is followed by oligomerization to nonvolatile form for monoterpenes, sesquiterpenes, isoprene, benzene, toluene, and xylene. Low-NO_x oxidation of aromatics leads to nonvolatile SOA. Glyoxal and methylglyoxal form SOA in clouds only.[55] Primary organic aerosol (POA) is tracked separately in terms of its carbon and noncarbon content, and functionality is added to POA through heterogeneous reactions with OH[56] (Figure S1).

In addition to the standard treatment of SOA in CMAQ v5.0.2, formation of SOA from IEPOX and MPAN oxidation products[57] was included in this work. To avoid double counting when pON aerosol was implemented, the Odum 2-product SOA from monoterpene + NO_3 reaction (using photooxidation SOA yields from Griffin et al.[44] daylight experiments) was removed. Double counting with the monoterpene photo-oxidation systems is expected to be minimal given the diurnal variation in pON (see Results section). Standard CMAQ v5.0.2 does not form SOA from isoprene + NO_3, but it was added using photooxidation yields for base simulations since other CMAQ v5.1 mechanisms include it. SOA from naphthalenes and alkanes[58] was not included.

In this work, SOA from isoprene- and monoterpene- derived organic nitrates (ISOPNN and $MTNO_3$ respectively) was implemented by treating them as semivolatile and allowing them to partition between the gas and aerosol phases (see figure associated with abstract and Figure S1). Thus, the aerosol treatment conserved mass with the gas-phase chemistry. Since the nitrate identity was retained, CMAQ provided an explicit prediction of particulate organic nitrate. Additional semivolatile species from monoterpene and isoprene + NO_3 reactions were not considered.

The volatility of ISOPNN was based on the work of Rollins et al.[43] and their simulations of environmental chamber experiments of isoprene + NO_3. SOA formation was primarily due to second generation nitrates and consistent with

DOI: 10.1021/acs.est.5b03738
Environ. Sci. Technol. 2015, 49, 14195−14203

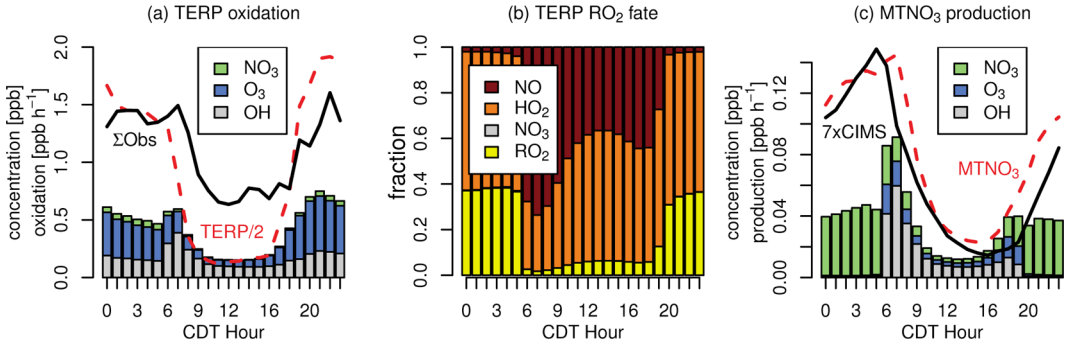

Figure 2. Predicted (a) oxidation of the lumped monoterpene, TERP, by oxidant, (b) monoterpene peroxy radical fate, and (c) production rate of $MTNO_3$ by oxidant during SOAS at CTR. Panel (a) includes the concentration of model species TERP (divided by two) and observed monoterpenes (other than α-pinene). Panel (c) includes the model predicted concentration of $MTNO_3$ and the concentration of C_{10} nitrates (multiplied by seven) observed by the Caltech CIMS.[67,68] τ = 3 h pseudohydrolysis.

partitioning of a C_5 dihydroxy dinitrate product with a molecular weight of 226 g mol^{-1}. A saturation concentration, C*, of 8.9 μg m^{-3} was assigned to ISOPNN based on Rollins et al.[43] though ISOPNN represents a number of compounds both more volatile and less volatile than the example structure.

$MTNO_3$ represented the entire class of monoterpene nitrates formed from all TERP reactions (both day and night and all RO_2 fates). Fry et al.[12] examined SOA from β-pinene + NO_3 and found that the ensemble of aerosol phase constituents could be modeled by assuming a 40−45% yield of gas-phase nitrates with a single vapor pressure. The vapor pressure that their model needed to fit the data is roughly consistent with a dihydroxy nitrate structure of molecular weight 231 g mol^{-1} and a saturation concentration of 12 μg m^{-3}. We applied this saturation concentration to all nitrates in $MTNO_3$ though multiple species with uncertain vapor pressures were represented by $MTNO_3$. An enthalpy of vaporization of 40 kJ mol^{-1} was used to adjust the saturation concentration of $MTNO_3$ and ISOPNN for different temperatures.[54]

A pseudohydrolysis reaction was implemented that converted particle-phase semivolatile organic nitrates to nitric acid and nonvolatile SOA (Table S3). While alcohols of similar volatility to their parent ON are a likely hydrolysis product, high molecular weight oligomers with one or two nitrate groups have also been observed in the particle.[59] The assumption of a nonvolatile hydrolysis product maximizes the amount of pON-derived SOA in the model. An effective time scale of 3 h, representative of tertiary nitrates,[16] was applied to all particle organic nitrates. Since Boyd et al.[16] estimate that only 10% of β-pinene + NO_3 nitrates are tertiary, a 30 h lifetime against pseudohydrolysis was also examined for greater consistency with the β-pinene data. However, limonene nitrates from NO_3 reaction are 60% tertiary based on SAPRC predictions. The 30 h lifetime was also consistent with the lifetime against oligomerization (29 h,[60]) implemented for all semivolatiles in CMAQ v5.0.2. Since the hydrolysis reaction results in a nonvolatile species and could encompass some accretion-like processes, we refer to it as pseudohydrolysis. The sum of particle-phase monoterpene nitrates, isoprene dinitrates, and their hydrolysis products are referred to as pON-derived aerosol.

Modeling studies[61−63] indicate glyoxal could be a significant SOA source. For completeness, SOA formation from glyoxal and methylglyoxal uptake to particles was added using an uptake coefficient of 2.9×10^{-3}.[63,64] This resulted in about 0.5 μg m^{-3} of OA for the SOAS site.

SOAS Field Observations. We focused our evaluation of CMAQ by comparing to measurements taken as part of the SOAS field campaign at CTR (32.90°N latitude, 87.25°W longitude). As part of SOAS, a high resolution time-of-flight aerosol mass spectrometer (HR-ToF-AMS) was operated by the Georgia Tech group.[4] Multivariate factor analysis with PMF identified subtypes of OA including LO-OOA. In addition, pON nitrate functional groups were estimated from the AMS data.[5] Since the AMS measures both organic and inorganic nitrate, the organic fraction was determined using the method of Farmer et al.[8] and the ratio of NO^+ to NO_2^+ fragments for organic nitrates (R_{ON}). Gas-phase NO_y and its speciation via thermo-photolysis and chemiluminescene were obtained as part of the SEARCH Network measurements.[65] Monoterpenes were measured via 2D-GC-FID.[66] In addition, the Caltech time-of-flight chemical ionization mass spectrometer (CIMS)[67] provided estimates of C_{10} multifunctional nitrates[68] at about 22 m above ground level. A table listing all measurements used in this work and additional model evaluation is provided in the Supporting Information. All comparisons to SOAS measurements used CMAQ predictions from the lowest model level (0 to about 20 m above ground level).

RESULTS

Spatial Distribution of pON-Derived Components. Particle-phase organic nitrogen from monoterpene oxidation was predicted to dominate over that from isoprene with CMAQ predicting a higher contribution from monoterpenes (>95%) than field modeling[4] (80%) suggests. Figure 1 shows the spatial distribution of SOA from monoterpene and isoprene nitrates as well as their organic hydrolysis product predicted for June 2013. Monoterpene nitrate SOA was predicted to be highest in the southeastern United States where monoterpene emissions are high. The highest $MTNO_3$ SOA concentrations occurred where NO_x sources were also large such as in urban areas, along highways, and near power plants. Isoprene nitrate SOA concentrations (Figure 1b) were lower reflecting the fact that most isoprene nitrates were expected to remain in the gas phase. Isoprene dominant regions were also shifted to the north of the monoterpene dominant region. With a 3 h lifetime of particulate organic nitrates against pseudohydrolysis, CMAQ predicted that the nonvolatile SOA from hydrolysis was roughly equal in magnitude to the prompt pON SOA from monoterpene oxidation (Figure 1c). As a result, biogenic volatile organic compound (BVOC) SOA (SOA from isoprene, monoterpenes, sesquiterpenes, and epoxides) was predicted to

DOI: 10.1021/acs.est.5b03738
Environ. Sci. Technol. 2015, 49, 14195−14203

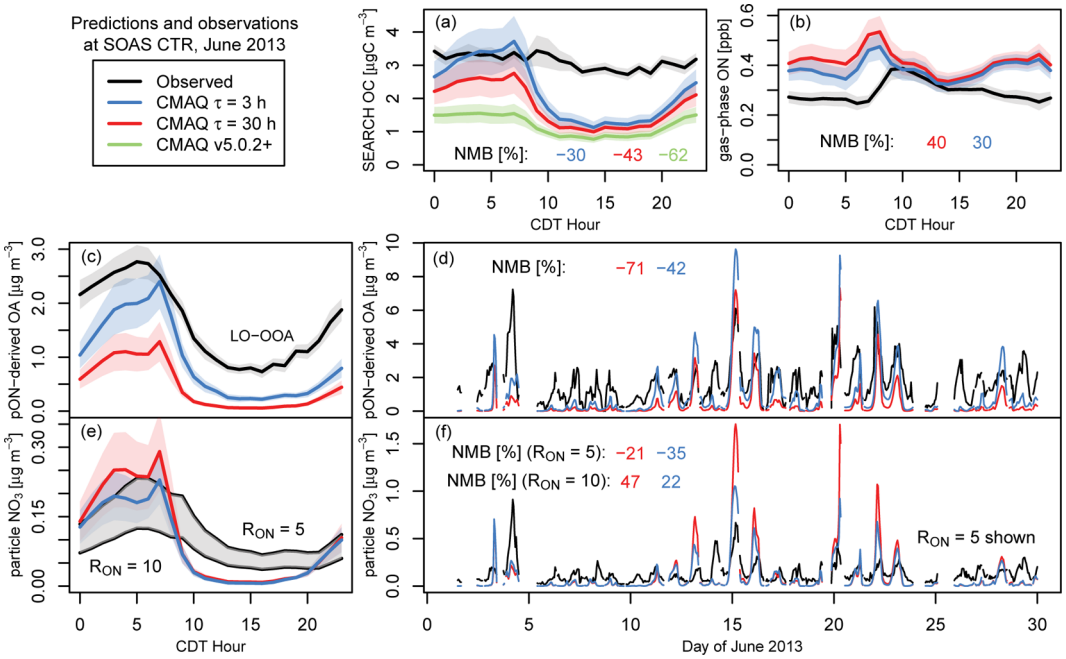

Figure 3. Predicted and observed (a) concentration of OC (SEARCH) (b) total gas-phase organic nitrates (SEARCH), (c,d) pON-derived SOA (LO-OOA from AMS measurements[4]), and (e,f) particle nitrate groups associated with organics (estimated from the AMS with R_{ON} = 5 and 10[5]) at Centreville SOAS site during June 2013. Predicted values are shown for the 3 h pseudohydrolysis lifetime (blue), 30 h pseudohydrolysis lifetime (red), and traditional CMAQ v5.0.2[54,56] with epoxide SOA[57] (green) where applicable. Updated CMAQ simulations include glyoxal/methylglyoxal SOA in addition to pON-derived SOA. The normalized mean bias (NMB) for each simulation (in percent) is shown in each panel. Shading indicates the standard error.

increase by as much as 2 μg m^{-3} on average (Figure 1d) compared to the CMAQ v5.0.2 + epoxide SOA scheme in which nitrate radical SOA was represented using photo-oxidation yields and an Odum 2-product approach. Even with the 30 h lifetime against pseudohydrolysis, BVOC SOA was predicted to increase by 0.5 μg m^{-3} over the base case in many areas since SOA yields from NO_3 oxidation are generally higher than those from OH or O_3 reaction (Figure S2).

Importance of Gas Phase in Determining pON-Derived SOA. The diurnal variation in model predicted pON-derived SOA was dictated by the production of gas-phase $MTNO_3$, boundary layer dynamics, and partitioning, all of which favored higher pON-derived aerosol concentrations at night. During the night, O_3 was the dominant TERP oxidant (Figure 2a) and was predicted to account for about 60% of TERP oxidation. NO_3 reaction accounted for about 10% of nocturnal TERP oxidation with the remaining 30% due to OH. The model was biased toward ozone and underestimated NO_3 oxidation as O_3 concentrations were high by 22% and NO_3[9] was low by 67% compared to measured values (Figure S7). OH[69,70] was reasonable (normalized mean bias: 7%) but overpredicted in the morning hours.

Predicted TERP concentrations exceeded the measured (via GC-MS[66]) sum of β-pinene, camphene, δ-limonene, and pcymene concentrations by roughly a factor of 2 at night. Predicted α-pinene concentrations were higher than observed by more than a factor of 2 at night consistent with the overprediction of NO_x (specifically NO_2, Figure S7) and potentially underestimated turbulent mixing at night. As monoterpenes are estimated to be the dominant sink of nitrate radicals at CTR during the night,[9] the high TERP and α-pinene levels likely contributed to the underestimated NO_3. Due to the low nitrate levels, the dominant monoterpene peroxy radical fate was reaction with HO_2 (accounting for about 60% of RO_2 reaction) followed by reaction with other RO_2 species (including all peroxy and acyl peroxy radical species except those from isoprene, Figures S8−S9) and small contributions from RO_2 + NO (Figure 2b). Even though $MTNO_3$ can form from ozonolysis and O_3 is the dominant TERP oxidant at night, the overwhelmingly dominant source of nocturnal monoterpene nitrates was TERP + NO_3 reaction since RO_2 + NO reaction was a small part of overall RO_2 fate. CMAQ predicted an average effective yield of 84% by mole for $MTNO_3$ from TERP + NO_3 at CTR, about 10% higher than the highest reported laboratory yields[14,15] and driven by the HO_2 pathway.

The model predicted concentration of pON-derived SOA was largest at 7 am CDT, just over an hour after sunrise. Moderate monoterpene concentrations combined with increasing OH, O_3, and RO_2 + NO made photooxidation the dominant source of monoterpene nitrates in the early morning (Figure 2c). The morning peak in production translated to a peak in predicted pON-derived aerosol.

Figure 2c also shows the sum of $C_{10}H_{17}NO_4$ and $C_{10}H_{17}NO_5$ measured by the Caltech CIMS instrument[68] which is about a factor of 7 lower than the model predicted $MTNO_3$. Although both these molecular formulas have been observed in laboratory generated β-pinene + NO_3 SOA,[16] $MTNO_3$ is a lumped surrogate nitrate representing all generations of monoterpene nitrates and thus contains monoterpene nitrates with less than 10 carbons as well as dinitrates and other multifunctional nitrates and agreement is not expected. In addition, the low model mixing may have led to higher than expected $MTNO_3$. But the nocturnal oxidation rate by NO_3 is expected to be more robust than TERP or NO_3 concentration predictions due to compensating effects (high TERP and low NO_3). Despite the difference in composition, the CIMS C_{10}

DOI: 10.1021/acs.est.5b03738
Environ. Sci. Technol. 2015, 49, 14195−14203

nitrate measurement and modeled $MTNO_3$ showed reasonable correlation (r^2 = 0.4).

Examination of Pseudohydrolysis Rate. The rate of organic nitrate pseudohydrolysis in the particle affected the magnitude and speciation of organic aerosol. Without the aerosol updates in this work (which included both pON-derived aerosol and glyoxal/methylglyoxal uptake to particles), CMAQ underestimated organic carbon in the particle at CTR by 62% (mean bias of 1.9 μg m^{-3}, Figure 3a). For τ = 30 h hydrolysis, model predictions were improved, particularly at night, and the overall underestimate reduced to 43%. For the fast hydrolysis simulation, OC (aerosol organic carbon) remained underestimated only during the day and early evening and by 30% overall. Total OA measured by the AMS was underestimated by 23% (1.3 μg m^{-3}). Note that the observed OC at CTR had a relatively flat diurnal profile as a result of a variety of sources and boundary layer dynamics,[4] and CMAQ continued to underestimate daytime OC levels. Fast hydrolysis reduced the model OC bias compared to the IMPROVE network[71] but degraded performance compared to CSN[71] (Table S9, Figure S10).

Figure 3c-d compares the slow (30 h) and fast (3 h) pseudohydrolysis scenarios in terms of the amount of pON-derived aerosol predicted. The AMS PMF factor, LO-OOA, was used as a surrogate for pON-derived aerosol and compared to the sum of monoterpene nitrate, isoprene nitrate, and hydrolysis product SOA predicted by the model. With the 30 h pseudohydrolysis, approximately 30% of LO-OOA was accounted for (mean bias −1.2 μg m^{-3}, normalized mean bias −71%, r^2 = 0.37). When the rate of hydrolysis was increased (τ = 3 h), the mean bias was reduced to −0.7 μg m^{-3} or −42% and the correlation improved (r^2 = 0.42), and approximately 60% of the observed LO-OOA was reproduced.

The nitrate functional groups attached to organics in the particle (Figure 3e,f) were estimated from AMS fragments and an R_{ON} (ratio of NO^+ to NO_2^+ fragments) of 5 and 10.[5] The slow hydrolysis simulation overestimated nitrate groups during the night and underestimated them during the day for both R_{ON} values. By increasing the hydrolysis rate, organic nitrates were effectively converted to nitric acid and the overestimate in organic particulate nitrate at night was reduced to a slight underestimate for R_{ON} = 5. For R_{ON} = 10, the fast hydrolysis simulation overestimated organic particulate nitrate at night and by 22% on average. The correlation between model predicted and observed pON-nitrates was not sensitive to the R_{ON} value and indicated both the fast and slow hydrolysis scenarios are consistent with the data (r^2 = 0.28 for τ = 30 h, r^2 = 0.33 for τ = 3 h).

During the day, CMAQ provided a reasonable simulation of the total gas-phase NO_y concentration and speciation (Figure S7). However, almost all NO_y components were significantly overestimated at night. Gas-phase organic nitrates, including monoterpene nitrates, isoprene nitrates, and other organic nitrates, were overestimated by 40% on average with the slow hydrolysis rate and 30% on average with the fast hydrolysis rate (Figure 3b). The largest improvements in gas-phase ON due to faster hydrolysis coincided with high pON at night. In addition to improving the gas-phase ON performance, fast hydrolysis also improved the NO_y estimate by about 20 ppt. As nitric acid was overestimated in the baseline simulation, faster hydrolysis exacerbated the overestimate in HNO_3 during SOAS. However, total inorganic nitrate (nitric acid + nitrate aerosol) in the South remained underestimated compared to CASTNET[72] observations (Figure S11).

Implications for Emission Reductions. Figure 4 shows the model-predicted speciation of organic aerosol at CTR. POA

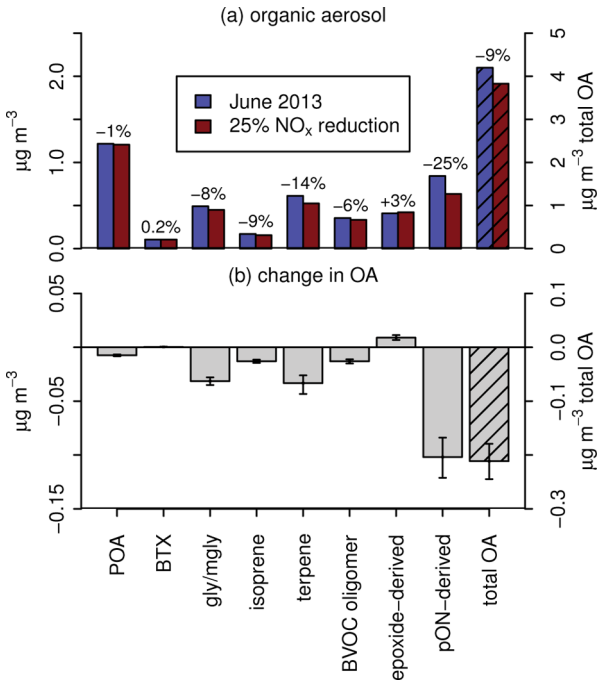

Figure 4. Predicted (a) mean OA concentration at CTR for June 2013 conditions and due to a 25% reduction in NO_x emissions. Each component is labeled with the percentage change in mean from the base simulation. Predicted (b) change in organic aerosol concentration and the 99% confidence interval (error bars) of the change estimated by a paired two-sided Wilcoxon signed rank test. All changes in panel (b) are statistically significant at the p = 0.01 level. Total OA concentration and change (diagonal stripes) are plotted on right vertical axis. τ = 3 h pseudohydrolysis.

was predicted to be a significant component of OA due to the nonvolatile nature of POA in the model. The second most abundant OA component was pON-derived SOA followed by terpene (monoterpene + sesquiterpene), glyoxal + methylglyoxal, and isoprene epoxide-derived SOA.

The Southeast has experienced large declines in NO_x emissions in the past few decades[1] as a result of regulations, and additional future declines in NO_x are expected.[73] To examine how the model responds to emission reductions, a simulation was conducted in which NO_x emissions from all sources were reduced by 25%. pON-derived SOA responded more strongly to NO_x emission reductions than any other component as NO_x has a direct role in formation of nitrate radicals and therefore monoterpene nitrate SOA. POA and single-ring aromatic (BTX) SOA showed very little response while all other components besides epoxide SOA showed a 6−14% decrease in mean concentration due to changes in oxidants (O_3, OH, NO_3). Epoxide-derived SOA was predicted to increase 3%, consistent with previous work[57] and changes in RO_2 fate. The overall effect of a 25% reduction in NO_x emissions was to reduce mean model predicted OA at CTR by 9%.

DOI: 10.1021/acs.est.5b03738
Environ. Sci. Technol. 2015, 49, 14195−14203

DISCUSSION

Multiple data sources[4,5,9] show a significant role for pON-derived SOA in the Southeast United States. The current SOA parametrization in CMAQ v5.0.2 and prior versions likely underestimates pON-derived SOA as a result of using photooxidation aerosol yields for nitrate radical reactions. In this work, we updated CMAQ to explicitly predict pON-derived SOA due to partitioning of gas-phase organic nitrates. We were able to account for no more than 60% of the LO-OOA factor and essentially all of the organic particulate nitrate at night with SOA from monoterpene and isoprene nitrates that react quickly (τ = 3 h) in the particle. While the model predictions of organic aerosol for the SOAS site were significantly improved compared to the base model in terms of magnitude and speciation, a number of questions and issues remain. The SOA yields as well as gas-phase $MTNO_3$ yields used here in CMAQ are already at or beyond the upper limit of those observed in chamber experiments for NO_3 reaction (Figure S2). By treating the hydrolysis product as nonvolatile, CMAQ has further maximized the amount of aerosol predicted from nitrogen-mediated processes. Particle-phase organic nitrate functional groups were captured relatively well at night but significantly underestimated during the day implying missing daytime sources. The magnitude of LO-OOA could be further improved by considering additional sources of LO-OOA such as ozonolysis, photooxidation, and pathways that do not contain nitrogen and should be explored in future work. The comparison of observed and modeled NO_y pointed to issues in the model at night potentially related to under-estimated turbulent mixing in the boundary layer, chemistry, and emissions. Thus, there is a critical need for additional laboratory and ambient data (e.g., in terms of aerosol volatility, concentration, etc.). A component of future analysis should include developing a mechanism for monoterpene oxidation that could be implemented in models since calculating SOA formation from monoterpene + nitrate radical reactions separately from gas-phase chemistry is not appropriate. Structure dependent and pH-dependent hydrolysis rate constants and the resulting product volatility for a range of organic nitrates from BVOC oxidation are also essential.

ASSOCIATED CONTENT

Supporting Information

The Supporting Information is available free of charge on the ACS Publications website at DOI: 10.1021/acs.est.5b03738.

Additional model documentation and evaluation (PDF) (TXT)

AUTHOR INFORMATION

Corresponding Author

*Phone: +1 (919)541-3557; e-mail: pye.havala@epa.gov.

Notes

The authors declare no competing financial interest.

ACKNOWLEDGMENTS

We thank Kristen Foley, Jon Pleim, Rohit Mathur, Kathleen Fahey, Rob Pinder, Ron Cohen, and Steve Brown for useful discussion. We thank CSC for emission processing, Shaojie Song for GEOS-Chem simulations, William Brune for OH observations, Tran Nguyen and Paul Wennberg (NSF grant AGS-1240604) for CIMS data, and William Brown for ceilometer data. We also thank the SOAS field team including Ann Marie Carlton. SEARCH is sponsored by Southern Company and EPRI. Georgia Tech was supported by NSF Grant 1242258 and U.S. EPA STAR RD-83540301 and R835410. J.L.F. acknowledges EPA STAR 83539901. P.B.S. acknowledges EPA STAR R835409. The U.S. EPA through its Office of Research and Development supported the research described here. It has been subjected to Agency administrative review and approved for publication, but may not necessarily reflect official Agency policy.

REFERENCES

(1) Hidy, G. M.; Blanchard, C. L.; Baumann, K.; Edgerton, E.; Tanenbaum, S.; Shaw, S.; Knipping, E.; Tombach, I.; Jansen, J.; Walters, J. Chemical climatology of the southeastern United States, 1999−2013. *Atmos. Chem. Phys.* **2014**, *14*, 11893−11914.

(2) Rollins, A. W.; Pusede, S.; Wooldridge, P.; Min, K. E.; Gentner, D. R.; Goldstein, A. H.; Liu, S.; Day, D. A.; Russell, L. M.; Rubitschun, C. L.; Surratt, J. D.; Cohen, R. C. Gas/particle partitioning of total alkyl nitrates observed with TD-LIF in Bakersfield. *J. Geophys. Res.-Atmos.* **2013**, *118*, 6651−6662.

(3) Fry, J. L.; et al. Observations of gas- and aerosol-phase organic nitrates at BEACHON-RoMBAS 2011. *Atmos. Chem. Phys.* **2013**, *13*, 8585−8605.

(4) Xu, L.; et al. Effects of anthropogenic emissions on aerosol formation from isoprene and monoterpenes in the southeastern United States. *Proc. Natl. Acad. Sci. U. S. A.* **2015**, *112*, 37−42.

(5) Xu, L.; Suresh, S.; Guo, H.; Weber, R. J.; Ng, N. L. Aerosol characterization over the southeastern United States using high-resolution aerosol mass spectrometry: spatial and seasonal variation of aerosol composition and sources with a focus on organic nitrates. *Atmos. Chem. Phys.* **2015**, *15*, 7307−7336.

(6) Day, D. A.; Liu, S.; Russell, L. M.; Ziemann, P. J. Organonitrate group concentrations in submicron particles with high nitrate and organic fractions in coastal southern California. *Atmos. Environ.* **2010**, *44*, 1970−1979.

(7) Rollins, A. W.; Browne, E. C.; Min, K. E.; Pusede, S. E.; Wooldridge, P. J.; Gentner, D. R.; Goldstein, A. H.; Liu, S.; Day, D. A.; Russell, L. M.; Cohen, R. C. Evidence for NO_x Control over Nighttime SOA Formation. *Science* **2012**, *337*, 1210−1212.

(8) Farmer, D. K.; Matsunaga, A.; Docherty, K. S.; Surratt, J. D.; Seinfeld, J. H.; Ziemann, P. J.; Jimenez, J. L. Response of an aerosol mass spectrometer to organonitrates and organosulfates and implications for atmospheric chemistry. *Proc. Natl. Acad. Sci. U. S. A.* **2010**, *107*, 6670−6675.

(9) Ayres, B. R.; et al. Organic nitrate aerosol formation via NO_3 + BVOC in the Southeastern US. *Atmos. Chem. Phys. Discuss.* **2015**, *15*, 16235−16272.

(10) Pye, H. O. T.; Chan, A. W. H.; Barkley, M. P.; Seinfeld, J. H. Global modeling of organic aerosol: the importance of reactive nitrogen (NO_x and NO_3). *Atmos. Chem. Phys.* **2010**, *10*, 11261−11276.

(11) Hoyle, C. R.; Berntsen, T.; Myhre, G.; Isaksen, I. S. A. Secondary organic aerosol in the global aerosol - chemical transport model Oslo CTM2. *Atmos. Chem. Phys.* **2007**, *7*, 5675−5694.

(12) Fry, J. L.; Kiendler-Scharr, A.; Rollins, A. W.; Wooldridge, P. J.; Brown, S. S.; Fuchs, H.; Dubé, W.; Mensah, A.; dal Maso, M.; Tillmann, R.; Dorn, H. P.; Brauers, T.; Cohen, R. C. Organic nitrate and secondary organic aerosol yield from NO_3 oxidation of β-pinene evaluated using a gas-phase kinetics/aerosol partitioning model. *Atmos. Chem. Phys.* **2009**, *9*, 1431−1449.

(13) Fry, J. L.; Kiendler-Scharr, A.; Rollins, A. W.; Brauers, T.; Brown, S. S.; Dorn, H. P.; Dubé, W. P.; Fuchs, H.; Mensah, A.; Rohrer, F.; Tillmann, R.; Wahner, A.; Wooldridge, P. J.; Cohen, R. C. SOA from limonene: role of NO_3 in its generation and degradation. *Atmos. Chem. Phys.* **2011**, *11*, 3879−3894.

(14) Spittler, M.; Barnes, I.; Bejan, I.; Brockmann, K. J.; Benter, T.; Wirtz, K. Reactions of NO_3 radicals with limonene and α-pinene: product and SOA formation. *Atmos. Environ.* **2006**, *40*, 116−127.

DOI: 10.1021/acs.est.5b03738
Environ. Sci. Technol. 2015, 49, 14195−14203

(15) Hallquist, M.; Wängberg, I.; Ljungström, E.; Barnes, I.; Becker, K.-H. Aerosol and product yields from NO_3 radical-initiated oxidation of selected monoterpenes. *Environ. Sci. Technol.* **1999**, *33*, 553−559.
(16) Boyd, C. M.; Sanchez, J.; Xu, L.; Eugene, A. J.; Nah, T.; Tuet, W. Y.; Guzman, M. I.; Ng, N. L. Secondary organic aerosol formation from the β-pinene + NO_3 system: effect of humidity and peroxy radical fate. *Atmos. Chem. Phys.* **2015**, *15*, 7497−7522.
(17) Perring, A. E.; Pusede, S. E.; Cohen, R. C. An observational perspective on the atmospheric impacts of alkyl and multifunctional nitrates on ozone and secondary organic aerosol. *Chem. Rev.* **2013**, *113*, 5848−5870.
(18) Browne, E. C.; Wooldridge, P. J.; Min, K. E.; Cohen, R. C. On the role of monoterpene chemistry in the remote continental boundary layer. *Atmos. Chem. Phys.* **2014**, *14*, 1225−1238.
(19) Hildebrandt Ruiz, L.; Yarwood, G. *Interactions between organic aerosol and NO_y: influence on oxidant production*, AQRP Project 12−012; Report, 2013, aqrp.ceer.utexas.edu/projectinfoFY12_13/12-012/12-012%20Final%20Report.pdf.
(20) Liu, S.; Shilling, J. E.; Song, C.; Hiranuma, N.; Zaveri, R. A.; Russell, L. M. Hydrolysis of organonitrate functional groups in aerosol particles. *Aerosol Sci. Technol.* **2012**, *46*, 1359−1369.
(21) Darer, A. I.; Cole-Filipiak, N. C.; O'Connor, A. E.; Elrod, M. J. Formation and stability of atmospherically relevant isoprene-derived organosulfates and organonitrates. *Environ. Sci. Technol.* **2011**, *45*, 1895−1902.
(22) Hu, K. S.; Darer, A. I.; Elrod, M. J. Thermodynamics and kinetics of the hydrolysis of atmospherically relevant organonitrates and organosulfates. *Atmos. Chem. Phys.* **2011**, *11*, 8307−8320.
(23) Russell, L. M.; Bahadur, R.; Ziemann, P. J. Identifying organic aerosol sources by comparing functional group composition in chamber and atmospheric particles. *Proc. Natl. Acad. Sci. U. S. A.* **2011**, *108*, 3516−3521.
(24) Rindelaub, J. D.; McAvey, K. M.; Shepson, P. B. The photochemical production of organic nitrates from α-pinene and loss via acid-dependent particle phase hydrolysis. *Atmos. Environ.* **2015**, *100*, 193−201.
(25) Blanchard, C. L.; Hidy, G. M.; Tanenbaum, S.; Edgerton, E. S.; Hartsell, B. E. The Southeastern Aerosol Research and Characterization (SEARCH) study: spatial variations and chemical climatology, 1999−2010. *J. Air Waste Manage. Assoc.* **2013**, *63*, 260−275.
(26) Washenfelder, R. A.; et al. Biomass burning dominates brown carbon absorption in the rural southeastern United States. *Geophys. Res. Lett.* **2015**, *42*, 653−664.
(27) Foley, K. M.; Roselle, S. J.; Appel, K. W.; Bhave, P. V.; Pleim, J. E.; Otte, T. L.; Mathur, R.; Sarwar, G.; Young, J. O.; Gilliam, R. C.; Nolte, C. G.; Kelly, J. T.; Gilliland, A. B.; Bash, J. O. Incremental testing of the Community Multiscale Air Quality (CMAQ) modeling system version 4.7. *Geosci. Model Dev.* **2010**, *3*, 205−226.
(28) Skamarock, W. C.; Klemp, J. B.; Dudhia, J.; Gill, D. O.; Barker, D. M.; Duda, M. G.; Huang, X.-Y.; Wang, W.; Powers, J. G. A description of the advanced research WRF version 3; Report, 2008.
(29) Henderson, B. H.; Akhtar, F.; Pye, H. O. T.; Napelenok, S. L.; Hutzell, W. T. A database and tool for boundary conditions for regional air quality modeling: description and evaluation. *Geosci. Model Dev.* **2014**, *7*, 339−360.
(30) Nolte, C. G.; Appel, K. W.; Kelly, J. T.; Bhave, P. V.; Fahey, K. M.; Collett, J. L., Jr; Zhang, L.; Young, J. O. Evaluation of the Community Multiscale Air Quality (CMAQ) model v5.0 against size-resolved measurements of inorganic particle composition across sites in North America. *Geosci. Model Dev.* **2015**, *8*, 2877−2892.
(31) Sarwar, G.; Gantt, B.; Schwede, D.; Foley, K. M.; Mathur, R.; Saiz-Lopez, A. Impact of enhanced ozone deposition and halogen chemistry on tropospheric ozone over the Northern Hemisphere. *Environ. Sci. Technol.* **2015**, *49*, 9203−9211.
(32) United States Environmental Protection Agency, *2011 National Emissions Inventory*, version 1 Technical Support Document; Report, **2013**, www3.epa.gov/ttn/chief/net/2011nei/2011_neiv1_tsd_draft.pdf.
(33) Farkas, C. M.; Moeller, M. D.; Felder, F. A.; Baker, K. R.; Rodgers, M.; Carlton, A. G. Temporalization of peak electric generation particulate matter emissions during high energy demand days. *Environ. Sci. Technol.* **2015**, *49*, 4696−4704.
(34) Carlton, A. G.; Baker, K. R. Photochemical modeling of the Ozark isoprene volcano: MEGAN, BEIS, and their impacts on air quality predictions. *Environ. Sci. Technol.* **2011**, *45*, 4438−4445.
(35) Bash, J. O.; Baker, K. R.; Beaver, M. R. Evaluation of improved land use and canopy representation in BEIS v3.61 with biogenic VOC measurements in California. *Geosci. Model Dev. Discuss.* **2015***8*, 8117−8154.10.5194/gmdd-8-8117-2015
(36) Xie, Y.; Paulot, F.; Carter, W. P. L.; Nolte, C. G.; Luecken, D. J.; Hutzell, W. T.; Wennberg, P. O.; Cohen, R. C.; Pinder, R. W. Understanding the impact of recent advances in isoprene photooxidation on simulations of regional air quality. *Atmos. Chem. Phys.* **2013**, *13*, 8439−8455.
(37) Lin, Y.-H.; et al. Epoxide as a precursor to secondary organic aerosol formation from isoprene photooxidation in the presence of nitrogen oxides. *Proc. Natl. Acad. Sci. U. S. A.* **2013**, *110*, 6718−6723.
(38) Hutzell, W. T.; Luecken, D. J.; Appel, K. W.; Carter, W. P. L. Interpreting predictions from the SAPRC07 mechanism based on regional and continental simulations. *Atmos. Environ.* **2012**, *46*, 417−429.
(39) Carter, W. P. L. Development of the SAPRC-07 chemical mechanism. *Atmos. Environ.* **2010**, *44*, 5324−5335.
(40) Carter, W. P. L. *Development of the SAPRC-07 Chemical Mechanism and Updated Ozone Reactivity Scales*, Final report to the California Air Resources Board Contract No. 03−318. January 27, 2010, www.cert.ucr.edu/~carter/SAPRC.
(41) Lee, L.; Teng, A. P.; Wennberg, P. O.; Crounse, J. D.; Cohen, R. C. On rates and mechanisms of OH and O_3 reactions with isoprene-derived hydroxy nitrates. *J. Phys. Chem. A* **2014**, *118*, 1622−1637.
(42) Crounse, J. D.; Knap, H. C.; Ornso, K. B.; Jorgensen, S.; Paulot, F.; Kjaergaard, H. G.; Wennberg, P. O. Atmospheric fate of methacrolein. 1. peroxy radical isomerization following addition of OH and O_2. *J. Phys. Chem. A* **2012**, *116*, 5756−5762.
(43) Rollins, A. W.; Kiendler-Scharr, A.; Fry, J. L.; Brauers, T.; Brown, S. S.; Dorn, H. P.; Dubé, W. P.; Fuchs, H.; Mensah, A.; Mentel, T. F.; Rohrer, F.; Tillmann, R.; Wegener, R.; Wooldridge, P. J.; Cohen, R. C. Isoprene oxidation by nitrate radical: alkyl nitrate and secondary organic aerosol yields. *Atmos. Chem. Phys.* **2009**, *9*, 6685−6703.
(44) Griffin, R. J.; Cocker, D. R.; Flagan, R. C.; Seinfeld, J. H. Organic aerosol formation from the oxidation of biogenic hydrocarbons. *J. Geophys. Res.* **1999**, *104*, 3555−3567.
(45) Fry, J. L.; Draper, D. C.; Barsanti, K. C.; Smith, J. N.; Ortega, J.; Winkler, P. M.; Lawler, M. J.; Brown, S. S.; Edwards, P. M.; Cohen, R. C.; Lee, L. Secondary organic aerosol formation and organic nitrate yield from NO_3 oxidation of biogenic hydrocarbons. *Environ. Sci. Technol.* **2014**, *48*, 11944−11953.
(46) Nguyen, T. B.; Crounse, J. D.; Schwantes, R. H.; Teng, A. P.; Bates, K. H.; Zhang, X. St.; Clair, J. M.; Brune, W. H.; Tyndall, G. S.; Keutsch, F. N.; Seinfeld, J. H.; Wennberg, P. O. Overview of the Focused Isoprene eXperiment at the California Institute of Technology (FIXCIT): mechanistic chamber studies on the oxidation of biogenic compounds. *Atmos. Chem. Phys.* **2014**, *14*, 13531−13549.
(47) Perraud, V.; Bruns, E. A.; Ezell, M. J.; Johnson, S. N.; Yu, Y.; Alexander, M. L.; Zelenyuk, A.; Imre, D.; Chang, W. L.; Dabdub, D.; Pankow, J. F.; Finlayson-Pitts, B. J. Nonequilibrium atmospheric secondary organic aerosol formation and growth. *Proc. Natl. Acad. Sci. U. S. A.* **2012**, *109*, 2836−2841.
(48) Jenkin, M. E.; Saunders, S. M.; Pilling, M. J. The tropospheric degradation of volatile organic compounds: a protocol for mechanism development. *Atmos. Environ.* **1997**, *31*, 81−104.
(49) Saunders, S. M.; Jenkin, M. E.; Derwent, R. G.; Pilling, M. J. Protocol for the development of the Master Chemical Mechanism, MCM v3 (Part A): tropospheric degradation of non-aromatic volatile organic compounds. *Atmos. Chem. Phys.* **2003**, *3*, 161−180.
(50) Mao, J.; Paulot, F.; Jacob, D. J.; Cohen, R. C.; Crounse, J. D.; Wennberg, P. O.; Keller, C. A.; Hudman, R. C.; Barkley, M. P.;

DOI: 10.1021/acs.est.5b03738
Environ. Sci. Technol. 2015, 49, 14195−14203

Horowitz, L. W. Ozone and organic nitrates over the eastern United States: sensitivity to isoprene chemistry. *J. Geophys. Res.* **2013**, *118*, 11,256−11,268.
(51) Carter, W. P. L.; Heo, G. Development of revised SAPRC aromatics mechanisms. *Atmos. Environ.* **2013**, *77*, 404−414.
(52) Sarwar, G.; Simon, H.; Xing, J.; Mathur, R. Importance of tropospheric $ClNO_2$ chemistry across the Northern Hemisphere. *Geophys. Res. Lett.* **2014**, *41*, 4050−4058.
(53) Atkinson, R.; Baulch, D. L.; Cox, R. A.; Crowley, J. N.; Hampson, R. F.; Hynes, R. G.; Jenkin, M. E.; Rossi, M. J.; Troe, J. Evaluated kinetic and photochemical data for atmospheric chemistry: Volume I - gas phase reactions of O_x, HO_x, NO_x and SO_x species. *Atmos. Chem. Phys.* **2004**, *4*, 1461−1738.
(54) Carlton, A. G.; Bhave, P. V.; Napelenok, S. L.; Edney, E. D.; Sarwar, G.; Pinder, R. W.; Pouliot, G. A.; Houyoux, M. Model representation of secondary organic aerosol in CMAQv4.7. *Environ. Sci. Technol.* **2010**, *44*, 8553−8560.
(55) Carlton, A. G.; Turpin, B. J.; Altieri, K. E.; Seitzinger, S. P.; Mathur, R.; Roselle, S. J.; Weber, R. J. CMAQ model performance enhanced when in-cloud secondary organic aerosol is included: comparisons of organic carbon predictions with measurements. *Environ. Sci. Technol.* **2008**, *42*, 8798−8802.
(56) Simon, H.; Bhave, P. V. Simulating the degree of oxidation in atmospheric organic particles. *Environ. Sci. Technol.* **2012**, *46*, 331−9.
(57) Pye, H. O. T.; et al. Epoxide pathways improve model predictions of isoprene markers and reveal key role of acidity in aerosol formation. *Environ. Sci. Technol.* **2013**, *47*, 11056−11064.
(58) Pye, H. O. T.; Pouliot, G. A. Modeling the role of alkanes, polycyclic aromatic hydrocarbons, and their oligomers in secondary organic aerosol formation. *Environ. Sci. Technol.* **2012**, *46*, 6041−6047.
(59) Draper, D. C.; Farmer, D. K.; Desyaterik, Y.; Fry, J. L. A comparison of secondary organic aerosol (SOA) yields and composition from ozonolysis of monoterpenes at varying concentrations of NO_2. *Atmos. Chem. Phys. Discuss.* **2015**, *15*, 14923−14960.
(60) Kalberer, M.; Paulsen, D.; Sax, M.; Steinbacher, M.; Dommen, J.; Prevot, A. S. H.; Fisseha, R.; Weingartner, E.; Frankevich, V.; Zenobi, R.; Baltensperger, U. Identification of polymers as major components of atmospheric organic aerosols. *Science* **2004**, *303*, 1659−1662.
(61) Ying, Q.; Li, J.; Kota, S. H. Significant contributions of isoprene to summertime secondary organic aerosol in Eastern United States. *Environ. Sci. Technol.* **2015**, *49*, 7834−7842. PMID: 26029963.
(62) Woo, J. L.; McNeill, V. F. simpleGAMMA v1.0 - a reduced model of secondary organic aerosol formation in the aqueous aerosol phase (aaSOA). *Geosci. Model Dev.* **2015**, *8*, 1821−1829.
(63) Fu, T.-M.; Jacob, D. J.; Wittrock, F.; Burrows, J. P.; Vrekoussis, M.; Henze, D. K. Global budgets of atmospheric glyoxal and methylglyoxal, and implications for formation of secondary organic aerosols. *J. Geophys. Res.* **2008**, *113*, D15303.
(64) Liggio, J.; Li, S.-M.; McLaren, R. Reactive uptake of glyoxal by particulate matter. *J. Geophys. Res.* **2005**, *110*, D10304.
(65) Wild, R. J.; Edwards, P. M.; Dubé, W. P.; Baumann, K.; Edgerton, E. S.; Quinn, P. K.; Roberts, J. M.; Rollins, A. W.; Veres, P. R.; Warneke, C.; Williams, E. J.; Yuan, B.; Brown, S. S. A measurement of total reactive nitrogen, NO_y, together with NO_2, NO, and O_3 via cavity ring-down spectroscopy. *Environ. Sci. Technol.* **2014**, *48*, 9609−9615.
(66) McAvey, K. M. Studies of the interaction of biogenic volatile organic compounds and NO_x in forest environments. Purdue University Ph.D. thesis, 2015.
(67) Crounse, J. D.; McKinney, K. A.; Kwan, A. J.; Wennberg, P. O. Measurement of gas-phase hydroperoxides by chemical ionization mass spectrometry. *Anal. Chem.* **2006**, *78*, 6726−6732.
(68) Nguyen, T. B.; Crounse, J. D.; Teng, A. P. St.; Clair, J. M.; Paulot, F.; Wolfe, G. M.; Wennberg, P. O. Rapid deposition of oxidized biogenic compounds to a temperate forest. *Proc. Natl. Acad. Sci. U. S. A.* **2015**, *112*, E392−E401.
(69) Faloona, I.; Tan, D.; Lesher, R.; Hazen, N.; Frame, C.; Simpas, J.; Harder, H.; Martinez, M.; Di Carlo, P.; Ren, X.; Brune, W. A laser-induced fluorescence instrument for detecting tropospheric OH and HO_2: characteristics and calibration. *J. Atmos. Chem.* **2004**, *47*, 139−167.
(70) Mao, J.; et al. Insights into hydroxyl measurements and atmospheric oxidation in a California forest. *Atmos. Chem. Phys.* **2012**, *12*, 8009−8020.
(71) Solomon, P. A.; Crumpler, D.; Flanagan, J. B.; Jayanty, R. K. M.; Rickman, E. E.; McDade, C. E. U.S. national PM2.5 chemical speciation monitoring networks-CSN and IMPROVE: description of networks. *J. Air Waste Manage. Assoc.* **2014**, *64*, 1410−1438.
(72) Lavery, T. F.; Rogers, C. M.; Baumgardner, R.; Mishoe, K. P. Intercomparison of Clean Air Status and Trends Network nitrate and nitric acid measurements with data from other monitoring programs. *J. Air Waste Manage. Assoc.* **2009**, *59*, 214−226.
(73) U.S. Environmental Protection Agency. Technical support document (TSD) preparation of the emissions inventories for the version 6.1, 2011 emissions modeling platform; Report, 2014. www3.epa.gov/ttn/chief/emch/2011v6/2011v6.1_2018_2025_base_EmisMod_TSD_nov2014_v6.pdf.

DOI: 10.1021/acs.est.5b03738
Environ. Sci. Technol. 2015, 49, 14195−14203